ACS NANO

www.acsnano.org

ARTICLE

Inducing Transient Charge State of a Single Water Cluster on Cu(111) Surface

Yang Guo,[†] Zijing Ding,[†] Lihuan Sun,[†] Jianmei Li,[†] Sheng Meng,*[,†,‡] and Xinghua Lu*[,†,‡]

[†]Beijing National Laboratory for Condensed-Matter Physics and Institute of Physics, Chinese Academy of Sciences, Beijing 100190, People's Republic of China

[‡]Collaborative Innovation Center of Quantum Matter, Beijing 100190, People's Republic of China

Supporting Information

ABSTRACT: **The hydrated electron on solid surface is a crucial species to interfacial chemistry. We present a joint low-temperature scanning tunneling microscopy and density functional theory investigation to explore the existence of a transient hydrated electron state induced by injecting tunneling electrons into a single water nonamer cluster on Cu(111) surface. The directional diffusion of water cluster under the Coulomb repulsive potential has been observed as evidence for the emergence of the transient hydrated electron. A critical structure transformation in water cluster for the emergence of hydrated electron has been identified. A charging mechanism has been proposed based on density functional theory calculation and scanning tunneling microscope results.**

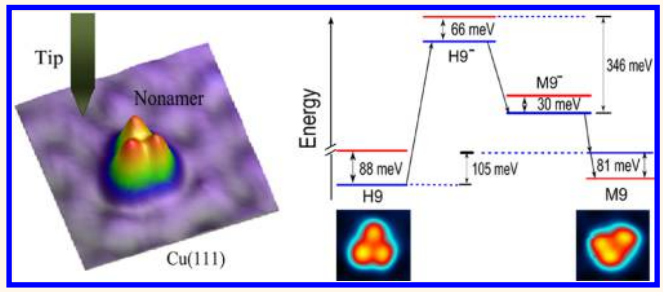

KEYWORDS: *hydrated electron, water cluster, charge state, Cu(111) surface, scanning tunneling microscopy, density functional theory*

An excess electron can be trapped in a nanostructure consisting of a few water molecules, resulting in a localized charge state called solvated electron or hydrated electron.[1−5] Hydrated electron plays a key role in physics and chemistry, and it has been implicated in a wide variety of phenomena in biology such as genetic damage.[6−8] Since its discovery in 1962, hydrated electron has attracted extensive investigations, and significant progress has been made in probing the structure and dynamics of this fascinating state,[9−17] mostly by spectroscopy on vapor/liquid phase water. It has been suggested, by vibrational spectra, that the excess electron binds to a double-acceptor (AA) molecule which accepts two hydrogen bonds from adjacent molecules but does not donate any hydrogen bond to the others. Pump−probe experiments also reveal that the excited-state lifetime of the hydrated electron in bulk water and isolated water clusters lies in the range from tens of femtosecond to picoseconds.[11−13] Real-space imaging of hydrated electrons, however, has not been possible, and very little is known about hydrated electrons on solid interfaces at the microscale which are relevant to a broad range of physicochemical phenomena and technological processes such as corrosion, lubrication, heterogeneous catalysis and electrochemistry. Even though neutral water clusters on various metal surfaces have been probed by scanning tunneling microscope (STM) for a long time, charged state of water cluster on surface has not been reported yet, mainly because of the strong screening effect of the conducting substrates.

Although the hydrated electron is not a lowest-energy stable state on metal surfaces, a transient charge state can be induced by injecting electrons to the water clusters on a surface with an STM tip. Here, we present our investigation on this transient charge state of water cluster on Cu(111) surface, by employing a low-temperature STM and first-principle density functional theory (DFT) calculations. With unique capabilities of STM,[18−21] we are able to image the structure of individual neutral water clusters, induce the transient charge state, and illustrate the signatures of charged water clusters. The structure of water clusters from DFT calculation explains well the observed changes in cluster conformation after the transient charge injection. In addition, a charging−discharging reaction path is proposed based on the results of both experiments and theoretical calculations.

RESULTS AND DISCUSSION

Individual water molecules are mobile on Cu(111) surface at temperature of 10 K;[22−24] they start to form clusters after a period of hours after deposition that are thermally stable for STM imaging, typically at sample bias of 20 mV and tunneling current of 10 pA. Figure 1a presents a typical STM image of such clusters on Cu(111) surface with ∼5% monolayer water coverage. Water clusters are shown as protrusions in the image. The basic building block of water clusters is the cyclic hexamer $(H_2O)_6$ with a 6-fold symmetric structure. As previously

Received: January 11, 2016
Accepted: March 23, 2016
Published: March 23, 2016

DOI: 10.1021/acsnano.6b00230
ACS Nano 2016, 10, 4489−4495

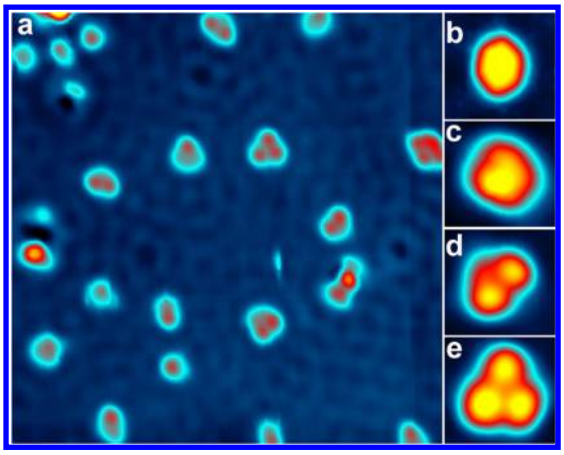

Figure 1. (a) STM image of water clusters on Cu(111) surface. Image size: 20 × 20 nm^2. Image is taken under sample bias of 20 mV and tunneling current of 10 pA. (b–e) STM images of single water cluster of different sizes: hexamer (b), heptamer (c), octamer (d), and nonamer (e). Image size: 2 × 2 nm^2.

revealed by Michaelides and Morgenstern,[25,26] the hexamers on Cu(111) surface prefer a buckled bilayer structure. And a hexamer can be hydrated by one, two, or three additional water molecules leading to heptamer $(H_2O)_7$, octamer $(H_2O)_8$, and nonamer $(H_2O)_9$. Figure 1b–e presents high-resolution topographs of water clusters from hexamer (b) to nonamer (e), as observed in our experiment. The additional water molecules in heptamers, octamers, and nonamers are clearly resolved as bright lobes. For example, the topograph of nonamer shows three bright lobes arranged in a regular triangle.

These water clusters on Cu(111) surface are neutral due to strong screening effect of the conducting metal substrate. To induce the charge state in a single water cluster, we positioned the STM tip aside a water cluster, turn off the feedback loop, increase the sample bias to a high voltage, and wait for a period of seconds before returning back to the normal scanning condition. The topograph taken after such an operation reveals a directional motion of the water cluster. Figure 2a–h presents a series of STM images illustrating such operation on a nonamer water cluster. The bright feature at the bottom left in each image is an atomic upper-terrace on Cu(111) surface, which is used as a reference object in image analysis. The position of STM tip during the voltage pulse operation is indicated by the yellow mark in each image, while the white arrow indicates the motion of the cluster after the voltage pulse. The water cluster always moves away from the tip center, and its structure is distorted from the original regular triangle. (The cluster in Figure 2a is not the original cluster before the first voltage pulse operation, and it is distorted as well.) To quantitatively explore the underlying mechanism, we performed the experiments with various bias voltage and current amplitude, and statistically measured the position of water clusters after each voltage pulse operation. For simplicity, we choose only nonamers to perform the operation since it is relatively easier to determine the center of the cluster. The same phenomena are observed on water clusters of different sizes as well. Panels i and j of Figure 2 present the distance (denoted as D) between tip and cluster after voltage pulse

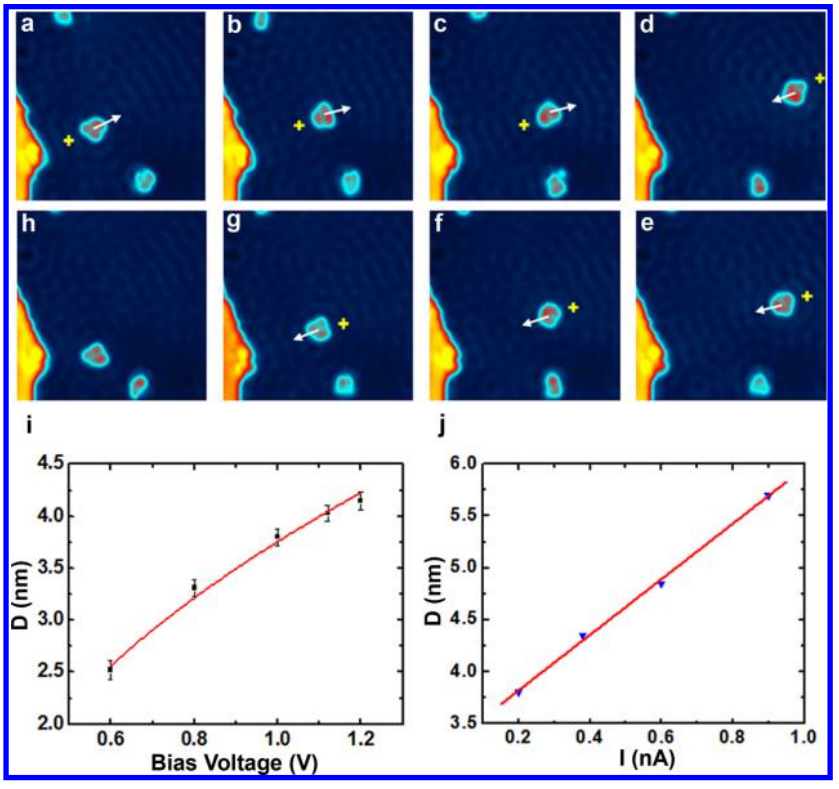

Figure 2. (a–h) Sequential STM images (15 × 15 nm^2) showing directional motion of a single nonamer on Cu(111) surface. Yellow crosses indicate the initial tip position and white arrows indicate the motion direction and distance. (i) The postdiffusion distance D as a function of sample bias voltage. The red curve corresponds to a polynomial fitting. (j) The postdiffusion distance D as a function of the tunneling current amplitude. Sample bias voltage is 1.0 V. The red line represents a linear fitting.

DOI: 10.1021/acsnano.6b00230
ACS Nano 2016, 10, 4489–4495

operations as a function of bias voltage and tunneling current amplitude, respectively. Each data point was statistically analyzed from about tens of operations. The error bars on Figure 2i indicate the mean square deviation at each operation condition. The relation between distance D and tunneling current amplitude is linear, while nonlinearity is apparent as the bias voltage varies. We note that the postdiffusion distance D does not depend on the initial distance between the tip and the cluster, as long as it is within a specific range. For negative sample bias, the water clusters move away from the tip center too, but the diffusion distance D depends weakly on the voltage amplitude (see Supporting Information Figure S1).

We attribute the observed directional motion of water cluster to the consequence of transient Coulomb repulsive interaction, although there are many other methods and mechanisms that may result in the motion of molecules on surface, including STM tip manipulation,[27] thermal diffusion, dipole interactions,[28] electronic excitation,[29] photoexcitation,[30] and static Coulomb force. We can easily exclude the possibility of tip manipulation and photoexcitation since the STM tip in our experiment is stationary and there is no light illumination. The effect of dipole interaction can be excluded as well since a polarized molecule always feels a lateral force pointing toward the center of the tip where the magnitude of electric field is highest, which is opposite to our observations. Pure electronic vibration excitation, which shall result in random diffusion,[28] cannot explain the directional motion of water cluster either. For a statically charged cluster, the direction of Coulomb force depends on the bias, and the clusters would diffuse toward the tip under negative sample bias, which is not supported by the observations. For a transient charge induced by the tunneling current, the charge (electron or hole) depends on the bias polarity (electron by positive sample bias and hole by negative sample bias) and always results in a repulsive Coulomb force. The above analysis and our experimental observation thus lead to a rational conclusion that the motion of water clusters is due to a transient Coulomb repulsive force when the clusters are charged during the voltage pulse operation. Due to the direct coupling of water clusters with the metallic surface, the lifetime of this charge state of water clusters is very short. We note that both the lowest unoccupied molecular orbital (LUMO) and the highest occupied molecular orbital (HOMO) of isolated water molecules are a few electronvolts away from the Fermi level. Inducing a hydrated electron state on surface, however, requires much less energy as the tail of LUMO state lies much closer to the Femi level due to the interaction with the electrons in the substrate. Considering the mechanism of excitation, the most plausible charging path is through inelastic tunneling electron excitation.[31] The interaction between water clusters on Cu(111) surface through the surface state was previously reported by Morgenstern and co-workers with the evidence of distance distribution oscillation.[32] In our study, we do observe the scattering of surface state by the water clusters, and the diffusion of the water cluster clearly alters the standing wave pattern. To minimize interactions between water clusters, we purposefully choose well-separated water clusters (at least several nanometers apart) in which the effect from cluster−cluster interaction is minor and ignorable. We also note that such phenomena has not been observed on other metal surfaces besides Cu(111).

To have a better understanding of this Coulomb repulsive force, we model the STM junction with a spherical conducting ball of radius R and a conducting flat surface. Then, the electrostatic potential energy near the surface can be express as $U(z, r) \sim \frac{2RzqV}{r^2 + 2HR}$, where H is the tunneling junction separation, z is the distance above the surface, q is the charge of the cluster, and V is the bias voltage (see Supporting Information for detailed derivation). When the water cluster is in charge neutral state, $q = 0$, the Coulomb potential exerts no force on the cluster. When the cluster is charged, however, it undertakes a significant Coulomb repulsive force. Assume that the cluster will stop at the position where the Coulomb potential equals the diffusion energy barrier ϕ along the surface, we get the relation between the bias voltage V and the final diffusion distance D, $V = \frac{\phi(D^2 + 2HR)}{2Rz|q|}$. Fitting the curve in Figure 2i with this function derives $HR = 2.4 \pm 0.5$ nm^2 and $\frac{\phi}{2Rz|q|} = 0.053 \pm 0.003$ V/nm^2. Taking the tunneling junction separation as 1 nm, the radius of curvature of the tip end R is about 2.4 nm. If we take the effective charge q as a unity of one electron and estimate the height of the water cluster to be 0.3 nm, then the diffusion energy barrier will be about 76 meV, which is on the same order of magnitude as derived from other experimental investigations.[22,23]

To reveal the detailed molecular structure of charged water clusters on Cu(111) surface, we carried out first-principle calculations within the framework of density functional theory (DFT). We first calculated the ground state of neutral water nonamers in various conformations without including the substrate. The most stable molecular structure of a neutral water nonamer is shown in Figure 3a, which has been

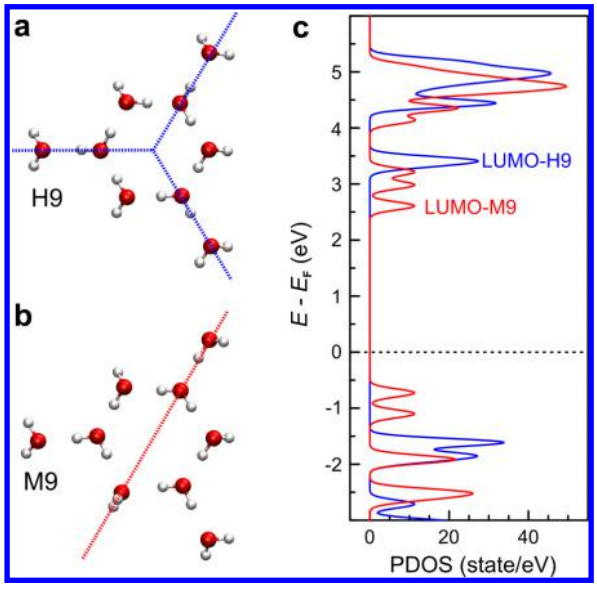

Figure 3. Geometric and electronic structures of model water clusters. (a) Homodromic structure (H9), (b) mirror symmetric structure (M9), and (c) density of states of H9 (blue curve) and M9 (red curve).

addressed in most of previous STM experiments and DFT calculations.[25,26] Such nonamer structure possesses six central H_2O molecules forming a cyclic homodromic hexamer, where each H_2O molecule acts as single H-bond donor and single H-bond acceptor. All the central six molecules are parallel to a same plane. Three additional H_2O molecules are linked to the central hexamer as H-bond acceptors. We denote this nonamer structure as 1,3,5-H9, where 1,3,5 indicates the positions of

DOI: 10.1021/acsnano.6b00230
ACS Nano 2016, 10, 4489−4495

three periphery H_2O molecules and H indicates the inner *homodromic* hexamer. The 1,3,5-H9 nonamer possesses a 3-fold rotational symmetry. The substrate-excluded electron density of state (DOS) in a 1,3,5-H9 nonamer is shown in Figure 3c. The energy levels are broadened to simulate the influence of the substrate, as explained later. By excluding the substrate in this calculation, we can survey tens of cluster conformations with reasonable computation time. In addition, it presents the electronic structure only of water clusters, which are helpful in identifying the corresponding states in the comprehensive substrate-included calculations. After identifying a few low-energy conformations, we added a five-layer 6 × 6 Cu(111) supercell to the model, simulating the influence of the substrate, to calculate more realistic electronic structures. Including substrate in the calculation results in the hybridization of states between water molecules and the copper atom. The splitting in molecular orbitals can be seen in the projected density of states (PDOS) of nonamers (see Supporting Information Figure S5). The broadening is about 0.2 eV, and such value is adopted in broadening the energy levels in Figure 3c.

In this study, we focus on the possibility of attaching electron to the water clusters. In a hydrogen bond network, each water molecule can simultaneously accept and donate two hydrogen bonds at most. In a 1,3,5-H9 nonamer, water molecules are divided into three groups: three one-acceptor-two-donor (ADD) molecules, three one-acceptor-one-donor (AD) molecules, and three one-acceptor (A) molecules. Since the extra electron tends to be doped into a LUMO state, we carefully examined the spatial distribution of LUMO state in various cluster conformations. Due to interaction with the substrate, the states are nondegenerate and we identify the LUMO state as the one with significant contribution from water molecules and the lowest energy among the split states. As shown in Figure 4a, we plot the LUMO state of 1,3,5-H9 nonamer on

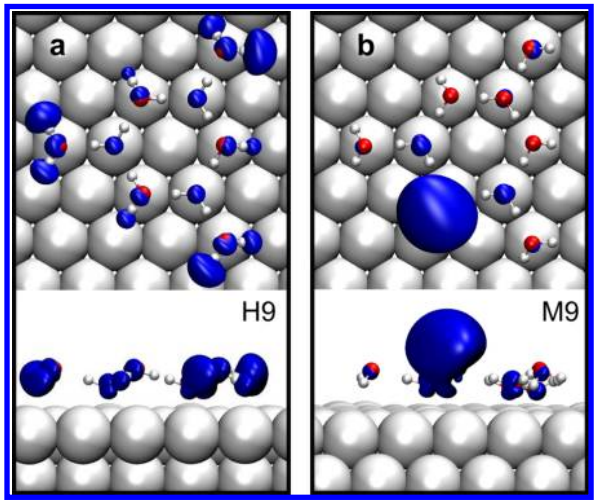

Figure 4. Top and side views of LUMO state in H9 (a) and M9 (b) nonamers on Cu(111) surface.

Cu(111) surface, which is distributed over all water molecules with slight difference reflecting variation in hydrogen bonding. We notice that the dangling hydrogen bond in a water cluster is closely associated with the LUMO wave function. This implies that an extra electron tends to be trapped by the dangling hydrogen bond. After surveying various other possibilities in arrangement of hydrogen bonds in a nonamer, we found an interesting structure in which one water molecule accepts two hydrogen bonds (double-acceptor, AA) but does not donate any hydrogen bond (with two dangling hydrogen bonds), as shown in Figure 3b. We denote this nonamer as 1,3,5-M9 since the central hexamer possess a *mirror* symmetry. The double-acceptor molecule lies along the symmetry line and perpendicular to the copper surface. The calculated density of states of a 1,3,5-M9 nonamer (red curve in Figure 3b) shows its LUMO energy of about 2.5 eV, significantly lower than that of a 1,3,5-H9 nonamer. It implies that M9 is easier to be charged by a low energy electronic excitation. Figure 4b shows the optimized geometry of 1,3,5-M9 on Cu(111) surface, as well as the spatial distribution of its LUMO state. It is clear that LUMO is localized at the double-acceptor water molecule, which looks like a half dumbbell. The localized LUMO state increases the possibility of accumulating excess electrons in an M9 nonamer. This result is very similar to that of gas-phase water cluster anions $(H_2O)^-_{4-6}$, where the electron is closely associated with a single water molecule attached to the H-bond network through a double H-bond acceptor motif.[11]

To explore the details in the charging process, we estimate energy of both neutral and charged H9 and M9 nonamers on Cu(111) surface with different arrangement of periphery molecules. The total electronic energy of a charged nonamer is calculated by adding the energy of corresponding neutral species on the surface and the LUMO energy (with respect to the Fermi level). Since the Coulomb energy is ignored with such treatment, the energy difference between a charged cluster and a neutral one is not accurate. However, the energy difference between charged species alone is believed to be reasonably accurate. It turns out that the 1,3,5-nonamer is more stable than 1,2,4-nonamer for the neutral H9, charged $H9^-$, and the charged $M9^-$. For neutral M9 nonamer, the 1,2,4-M9 configuration is more stable, 81 meV lower in total energy than that of 1,3,5-M9. Among all configurations we examined, 1,3,5-H9 is the most stable species. For charged species, 1,3,5-$M9^-$ is the most stable configuration, with an energy difference of 346 meV as compared to 1,3,5-$H9^-$. Experimentally, we noticed that most 1,3,5-nonamers are distorted after voltage pulse operation, resulting in a 1,2,4-nonamer configuration, as shown in Figure 5a. Combining the theoretical calculation results and experimental observations, we propose a plausible charging path in nonamer water clusters as follows: (1) the water molecules diffuse and aggregate into a neutral 1,3,5-H9 cluster on Cu(111) surface; (2) an electron is injected into 1,3,5-H9 cluster through inelastic tunneling, forming a charged 1,3,5-$H9^-$ cluster; (3) the interaction between the excess electron and the cluster phonon turns the cluster into a 1,3,5-$M9^-$, with the electron trapped to the double H-bond acceptor; (4) the excess electron transport to the conducting metal, leaving a neutral 1,3,5-M9 cluster on the surface; (5) the 1,3,5-M9 cluster relaxes to a lower-energy 1,2,4-M9 configuration.

The lifetime of the charged 1,3,5-$H9^-$ cluster is on the order of femtosecond, since it is just a pure electronic excitation on metal surface. Besides the transition back to the neutral 1,3,5-H9 state directly, the charged water cluster may also change its structure into 1,3,5-$M9^-$ configuration to embrace the excess electron, leading to the emergence of the hydrated electron state. The lifetime of this hydrated electron state is expected to be much longer, since the hydrated electron state in nature is a polaron resulting from the quantum coupling of the excess electron and molecular phonon. A lifetime of picoseconds for hydrated electrons in water clusters, in both gas phase and solid phase, has been reported by many previous studies.[10,12,13] We

DOI: 10.1021/acsnano.6b00230
ACS Nano 2016, 10, 4489−4495

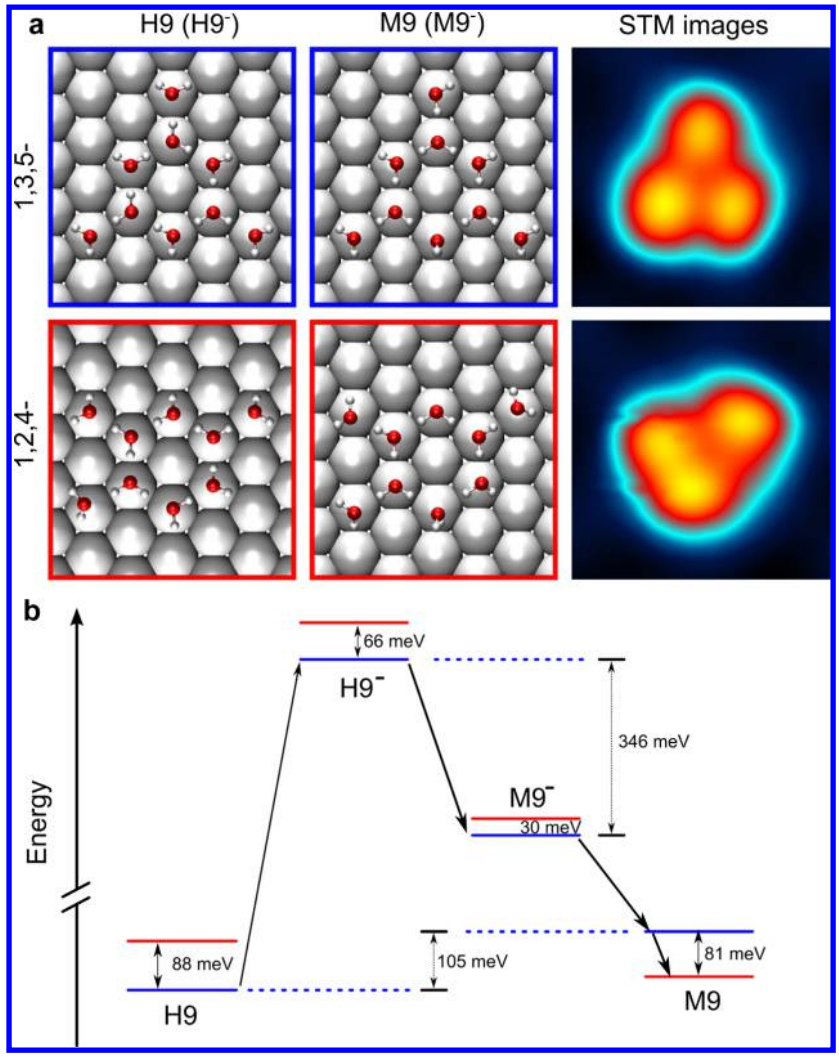

Figure 5. (a) Structure models of 1,3,5-nonamer and 1,2,4-nonamer clusters and the corresponding STM images (2.4 × 2.4 nm^2) of nonamers before and after excitation. (b) Energy alignments of H9/H9$^-$ and M9/M9$^-$ with 1,3,5-nonamer and 1,2,4-nonamer structure. Arrow indicates the most plausible charging path.

suggest that the structural transformation of water clusters on Cu(111) surface, from a homodromic structure to a mirror symmetric structure, is a critical step for trapping the excess electron, which results in the redistribution of hydrogen-bond network and the formation of new localized low-lying molecular orbitals in water clusters. The transition barrier energy between homodromic H6 and mirror symmetric M6 is about 0.52 eV, based on climbing image nudged elastic band (NEB) method calculation (see Supporting Information Figure S6).

When the excess electron transports to the conducting substrate, the resulting neutral 1,3,5-M9 cluster will relax to a lower-energy 1,2,4-M9 configuration. The activation energy for a peripheral water transfer from one site to another site on the underlying hexamer is about 0.29 eV, as derived in ref 24. The neutral 1,2,4-M9 cluster, being 24 meV higher in energy than the 1,3,5-H9, is a kinetically trapped state that is stable on surface during STM imaging. This is because of a high transition energy barrier between the two species. Consider thermodynamic stability, the 1,2,4-M9 cluster could restore to the 1,3,5-H9 structure if it is waited for longer time and the substrate temperature is raised; therefore, it is possible that the full cycle can be completed for water cluster manipulation. Given the conducting nature of metal substrate, the hydrated electron states induced on metal surfaces are surprising, and would be of fundamental importance to understand electronic processes in electrochemistry, water photocatalysis, and ice nucleation, as well as bringing new physics to water science and surface engineering.

CONCLUSIONS

In summary, we demonstrated directional manipulation of individual water cluster on Cu(111) surface through inelastic tunneling electron, and the existence of a transient charge state has been identified through the diffusion kinetics under the Coulomb repulsive potential. Combining DFT calculations and STM experimental results, the charging mechanism has been revealed at the atomic scale for generating hydrated electron in water cluster on metallic surface. Our findings provide fundamental information for future studies in detection and manipulation of hydrated electrons on water/solid interfaces.

EXPERIMENTAL SECTION

Our experiments were carried out in a home-built ultrahigh-vacuum (UHV) STM which is similar to that developed by B. C. Stipe *et al.* in Prof. Wilson Ho's research group.[33] The microscope utilizes a Besocke

DOI: 10.1021/acsnano.6b00230
ACS Nano 2016, 10, 4489−4495

"beetle" type scanner[34,35] and is well-suited for tunneling spectroscopy and manipulation for single molecule studies. The base pressure of the system is below 1×10^{-10} Torr and the operation temperature is around 10 K.[36] The single crystal Cu(111) was purchased from MaTecK GmbH. After thorough outgas at 500 K, the crystal surface was prepared by multiple cycles of Ar^+ sputtering (1 keV in energy and 5 min each cycle) and annealing at 800 K (500 K for the last cycle). The cleaned Cu(111) crystal was then transferred to the STM stage and cooled to around 10 K with liquid helium. Ultrapure water was obtained from Millipore Company and further purified by freeze−pump−thaw cycles using liquid nitrogen. The water vapor was then introduced into the UHV chamber *via* a leak valve and deposited straightly onto the surface of Cu(111) crystal in the cold STM stage. The water coverage varies between 2% and 20% in our experiments. There was no anneal performed after deposition of water clusters, and all STM manipulation and imaging were performed at the temperature around 10 K.

We carried out first-principle calculations within the framework of density functional theory (DFT), employing Projector-Augmented-Wave (PAW) pseudopotentials and the Perdew−Burke−Ernzerholf (PBE) form of the exchange-correlation functional,[37−39] as implemented in VASP code.[40] The substrate consists of five-layer Cu(111) atomic slabs with a lattice constant of 2.56 Å taken from experimental values. A Cu (6×6) supercell is used to accommodate the water nonamer. For gas phase water clusters, the structure and energetics are again checked against larger supercell size $30 \times 30 \times 20$ Å^3 to guarantee that the spurious Coulombic interaction between periodic images is negligible. We employ an energy cutoff of 400 eV for plane waves, and the criterion for total energy convergence is set to 10^{-4} eV. The density of states (DOS) in an isolated water clusters is broadened to simulate the interaction with the substrate.

ASSOCIATED CONTENT

Supporting Information

The Supporting Information is available free of charge on the ACS Publications website at DOI: 10.1021/acsnano.6b00230.

Diffusion behavior of water cluster as a function of sample bias voltage; electrostatic potential in an STM junction; influence of surface polarization and molecular cluster polarization; projected density of states (PDOS) of water clusters on Cu(111) surface; the transition barrier between water hexamer H6 and M6; and top view of several possible M9 arrangements (PDF)

AUTHOR INFORMATION

Corresponding Authors

*E-mail: smeng@iphy.ac.cn.
*E-mail: xhlu@iphy.ac.cn.

Notes

The authors declare no competing financial interest.

ACKNOWLEDGMENTS

This research is supported by Ministry of Science and Technology of China under Grant Nos. 2012CB933002 and 2012CB921403, National Science Foundation of China under Grant Nos. 11174347, 61027011, 11290164, and 61376100. Strategic Priority Research Program (B) of the Chinese Academy of Sciences, Grant No. XDB07030100. S. Meng and X. Lu thank the support of Hundred Talent Program of Chinese Academy of Sciences. We thank the assistance of Mr. Lailai Li and Mr. Dong Li in carrying out the STM experiments.

REFERENCES

(1) Weiss, J. Primary Processes in the Action of Ionizing Radiations on Water: Formation and Reactivity of Self-Trapped Electrons ('Polarons'). *Nature* **1960**, *186*, 751−752.
(2) Hart, E. J.; Boag, J. W. Absorption Spectrum of the Hydrated Electron in Water and in Aqueous Solutions. *J. Am. Chem. Soc.* **1962**, *84*, 4090−4095.
(3) Migus, A.; Gauduel, Y.; Martin, J. L.; Antonetti, A. Excess Electrons in Liquid Water: First Evidence of a Prehydrated State with Femtosecond Lifetime. *Phys. Rev. Lett.* **1987**, *58*, 1559−1562.
(4) Buxton, G. V.; Greenstock, C. L.; Helman, W. P.; Ross, A. B. Critical Review of Rate Constants for Reactions of Hydrated Electrons, Hydrogen Atoms and Hydroxyl Radicals(•OH/ $•O^-$) in Aqueous Solution. *J. Phys. Chem. Ref. Data* **1988**, *17*, 513−886.
(5) Jordan, K. D. A Fresh Look at Electron Hydration. *Science* **2004**, *306*, 618−619.
(6) Mezyk, S. P.; Neubauer, T. J.; Cooper, W. J.; Peller, J. R. Free-Radical-Induced Oxidative and Reductive Degradation of Sulfa Drugs in Water: Absolute Kinetics and Efficiencies of Hydroxyl Radical and Hydrated Electron Reactions. *J. Phys. Chem. A* **2007**, *111*, 9019−9024.
(7) Berdys, J.; Anusiewicz, I.; Skurski, P. Damage to Model DNA Fragments from Very Low-Energy (<1eV) Electrons. *J. Am. Chem. Soc.* **2004**, *126*, 6441−6447.
(8) Rezaee, M.; Sanche, L.; Hunting, D. J. Cisplatin Enhances the Formation of DNA Single- and Double-Strand Breaks by Hydrated Electrons and Hydroxyl Radicals. *Radiat. Res.* **2013**, *179*, 323−331.
(9) Lehr, L.; Zanni, M. T.; Frischkorn, C.; Weinkauf, R.; Neumark, D. M. Electron Solvation in Finite Systems: Femtosecond Dynamics of Iodide · $(Water)_n$ Anion Clusters. *Science* **1999**, *284*, 635−638.
(10) Gahl, C.; Bovensiepen, U.; Frischkorn, C.; Wolf, M. Ultrafast Dynamics of Electron Localization and Solvation in Ice Layers on Cu(111). *Phys. Rev. Lett.* **2002**, *89*, 107402.
(11) Hammer, N. I.; Shin, J.-W.; Headrick, J. M.; Diken, E. G.; Roscioli, J. R.; Weddle, G. H.; Johnson, M. A. How Do Small Water Clusters Bind an Excess Electron? *Science* **2004**, *306*, 675−679.
(12) Bragg, A. E.; Verlet, J. R. R.; Kammrath, A.; Cheshnovsky, O.; Neumark, D. M. Hydrated Electron Dynamics: From Clusters to Bulk. *Science* **2004**, *306*, 669−671.
(13) Paik, D. H.; Lee, I.-R.; Yang, D.-S.; Baskin, J. S.; Zewail, A. H. Electrons in Finite-Sized Water Cavities: Hydration Dynamics Observed in Real Time. *Science* **2004**, *306*, 672−675.
(14) Williams, C. F.; Herbert, J. M. Influence of Structure on Electron Correlation Effects and Electron-Water Dispersion Interactions in Anionic Water Clusters. *J. Phys. Chem. A* **2008**, *112*, 6171−6178.
(15) Young, R. M.; Neumark, D. M. Dynamics of Solvated Electrons in Clusters. *Chem. Rev.* **2012**, *112*, 5553−5577.
(16) Elkins, M. H.; Williams, H. L.; Shreve, A. T.; Neumark, D. M. Relaxation Mechanism of the Hydrated Electron. *Science* **2013**, *342*, 1496−1499.
(17) Lee, H. M.; Kim, K. S. Dynamics and Structural Changes of Small Water Clusters on Ionization. *J. Comput. Chem.* **2013**, *34*, 1589−1597.
(18) Crommie, M. F.; Lutz, C. P.; Eigler, D. M. Confinement of Electrons to Quantum Corrals on a Metal Surface. *Science* **1993**, *262*, 218−220.
(19) Nazin, G. V.; Qiu, X. H.; Ho, W. Visualization and Spectroscopy of a Metal-Molecule-Metal Bridge. *Science* **2003**, *302*, 77−81.
(20) Repp, J.; Meyer, G.; Olsson, F. E.; Persson, M. Controlling the Charge State of Individual Gold Adatoms. *Science* **2004**, *305*, 493−495.
(21) Liljeroth, P.; Repp, J.; Meyer, G. Current-Induced Hydrogen Tautomerization and Conductance Switching of Naphthalocyanine Molecules. *Science* **2007**, *317*, 1203−1206.
(22) Hodgson, A.; Haq, S. Water Adsorption and the Wetting of Metal Surfaces. *Surf. Sci. Rep.* **2009**, *64*, 381−451.
(23) Morgenstern, K.; Rieder, K.-H. Formation of the Cyclic Ice Hexamer *via* Excitation of Vibrational Molecular Modes by the Scanning Tunneling Microscope. *J. Chem. Phys.* **2002**, *116*, 5746−5752.

DOI: 10.1021/acsnano.6b00230
ACS Nano 2016, 10, 4489−4495

(24) Mehlhorn, M.; Carrasco, J.; Michaelides, A.; Morgenstern, K. Local Investigation of Femtosecond Laser Induced Dynamics of Water Nanoclusters on Cu(111). *Phys. Rev. Lett.* **2009**, *103*, 026101.
(25) Michaelides, A.; Morgenstern, K. Ice Nanoclusters at Hydrophobic Metal Surfaces. *Nat. Mater.* **2007**, *6*, 597−601.
(26) Carrasco, J.; Hodgson, A.; Michaelides, A. A Molecular Perspective of Water at Metal Interfaces. *Nat. Mater.* **2012**, *11*, 667−674.
(27) Gimzewski, J. K.; Joachim, C. Nanoscale Science of Single Molecules Using Local Probes. *Science* **1999**, *283*, 1683−1688.
(28) Yan, S. C.; Xie, N.; Gong, H. Q.; Sun, Q.; Guo, Y.; Shan, X. Y.; Lu, X. H. Mapping the Diffusion Potential of a Reconstructed Au(111) Surface at Nanometer Scale with 2D Molecular Gas. *Chin. Phys. Lett.* **2012**, *29*, 046803.
(29) Komeda, T.; Kim, Y.; Kawai, M.; Persson, B. N. J.; Ueba, H. Lateral Hopping of Molecules Induced by Excitation of Internal Vibration Mode. *Science* **2002**, *295*, 2055−2058.
(30) Bartels, L.; Wang, F.; Mö, D.; Knoesel, E.; Heinz, T. F. Real-Space Observation of Molecular Motion Induced by Femtosecond Laser Pulses. *Science* **2004**, *305*, 648−651.
(31) Gawronski, H.; Carrasco, J.; Michaelides, A.; Morgenstern, K. Manipulation and Control of Hydrogen Bond Dynamics in Absorbed Ice Nanoclusters. *Phys. Rev. Lett.* **2008**, *101*, 136102.
(32) Mehlhorna, M.; Simic-Milosevica, V.; Jakschb, S.; Scheierb, P.; Morgenstern, K. The influence of the surface state onto the distance distribution of single molecules and small molecular clusters. *Surf. Sci.* **2010**, *604*, 1698.
(33) Stipe, B. C.; Rezaei, M. A.; Ho, W. A variable-Temperature Scanning Tunneling Microscope Capable of Single-Molecule Vibrational Spectroscopy. *Rev. Sci. Instrum.* **1999**, *70*, 137−143.
(34) Besocke, K. An easily operable scanning tunneling microscope. *Surf. Sci.* **1987**, *181*, 145.
(35) Frohn, J.; Wolf, J. F.; Besocke, K.; Teske, M. Coarse tip distance adjustment and positioner for a scanning tunneling microscope. *Rev. Sci. Instrum.* **1989**, *60*, 1200.
(36) Yan, S.; Ding, Z.; Xie, N.; Gong, H.; Sun, Q.; Guo, Y.; Shan, X.; Meng, S.; Lu, X. Turning on and off the Rotational Oscillation of a Single Porphine Molecule by Molecular Charge State. *ACS Nano* **2012**, *6*, 4132−4136.
(37) Vanderbilt, D. Soft Self-Consistent Pseudopotentials in a Generalized Eigenvalue Formalism. *Phys. Rev. B: Condens. Matter Mater. Phys.* **1990**, *41*, 7892−7895.
(38) Blöchl, P. E. Projector Augmented-Wave Method. *Phys. Rev. B: Condens. Matter Mater. Phys.* **1994**, *50*, 17953−17979.
(39) Perdew, J. P.; Burke, K.; Ernzerhof, M. Generalized Gradient Approximation Made Simple. *Phys. Rev. Lett.* **1996**, *77*, 3865−3868.
(40) Kresse, G.; Hafner, J. *Ab initio* Molecular Dynamics for Liquid Metals. *Phys. Rev. B: Condens. Matter Mater. Phys.* **1993**, *47*, 558−561.

DOI: 10.1021/acsnano.6b00230
ACS Nano 2016, 10, 4489−4495